Available online at www.sciencedirect.com
SCIENCE DIRECT®
Journal of Catalysis 223 (2004) 372–381
JOURNAL OF CATALYSIS
www.elsevier.com/locate/jcat

New Pd/Pt on Mg/Al basic mixed oxides for the hydrogenation and hydrogenolysis of naphthalene

S. Albertazzi,[a] G. Busca,[b] E. Finocchio,[b] R. Glöckler,[c] and A. Vaccari [a,*]

[a] *Dipartimento di Chimica Industriale e dei Materiali, Università di Bologna, INSTM-UdR di Bologna, Viale Risorgimento, 4, 40136 Bologna, Italy*
[b] *Dipartimento di Ingegneria Chimica e di Processo, Università di Genova, INSTM-UdR di Genova, P. le Kennedy, 16129, Genova, Italy*
[c] *SASOL Germany GmbH, Fritz-Staiger Straße 15, 25541 Brunsbüttel, Germany*

Received 29 October 2003; accepted 25 January 2004

Abstract

New Pd/Pt catalysts supported on a basic Mg/Al mixed oxide obtained by calcination of a commercial hydrotalcite (SASOL, D) have been fully characterized by XRD, SEM, and FTIR and investigated in the vapor-phase hydrogenation of naphthalene in order to put in evidence the role of the Pd/Pt active phase and the acidity of the support on the hydrogenolysis/ring-opening reaction as well as the thio-tolerance of the catalysts. After calcination the hydrotalcite support (HT) gave rise to a Mg/Al mixed oxide with high surface area and a "brain-like" surface morphology. The IR spectra after adsorption of CO over the reduced samples showed the interaction between bimetallic particles and Mg–Al(O) basic support. The main band in the range 2080–2070 cm^{-1} is due to on-top CO adsorbed over Pd^0 or Pt^0, while the complex absorption below 2000 cm^{-1} is due to CO species bridging over Pd^0. All the samples showed mainly a hydrogenation activity, highlighting the role of the support acidity in the ring-opening reactions to high molecular weight (HMW) products, having a boosting effect on the cetane number of the fraction obtained. A significant increase in the amount of HMW products was obtained by decreasing the Pd/Pt ratio, showing also the role of hydrogenolysis reactions attributable mainly to Pt, thus suggesting a hydrogenolysis/ring-opening mechanism. Furthermore, the Pd/Pt on basic oxide catalysts did not give rise to useless low molecular weight (LMW) cracking compounds, which thus formed only on highly acid sites. Finally, these catalysts, investigated by feeding increasing amounts of dibenzothiophene (DBT), showed an almost constant activity up to 3000 wt ppm of DBT. This surprising result pointed out the intrinsic thio-resistance of the Pd/Pt pair, regardless of a possible contribution of the acid sites of the support, and is mainly attributed to its high hydrodesulfurization (HDS) activity.

Keywords: Hydrotalcite; Pd/Pt; Naphthalene; Hydrogenation; Hydrogenolysis/ring-opening; Cracking; Decahydronaphthalene; Tetrahydronaphthalene; CO adsorption; IR spectroscopy

1. Introduction

The removal of aromatic hydrocarbons and the increase of cetane number in diesel fuels have received considerable attention in recent years, due to the fact that environmental regulations governing the composition of diesel fuels are being tightened in both Europe and the United States [1,2]. In particular, a high aromatic content and a low cetane number worsen the quality of diesel fuel and increase the smoke point. Thus, the development of catalytic technology for aromatic saturation (HYD) and sulfur removal (HDS) is highly desirable. Two approaches are proposed in the literature for meeting the above requirements. A single-step process combines severe HDS with HYD and uses conventional hydrotreating catalysts, such as Ni–Mo and Ni–W sulfide on alumina and zeolites [3–6]. These catalysts have the advantage of high tolerance to sulfur in the feed, although the activity of a metal sulfide catalyst is not sufficient to reach the required aromatic saturation, so a high temperature is necessary. On the other hand, high temperatures thermodynamically inhibit the aromatic hydrogenation and this drawback may only be partially balanced by operating at high hydrogen partial pressure.

A two-step process uses a hydrotreating catalyst in the first reactor and a noble metal-containing catalyst in the second reactor, since noble metal catalysts are generally poisoned even by few wt ppm of sulfur in the feed [7,8]. Among them, a relatively high thio-tolerance has been recently reported for Pd, Pt, and, mainly, bimetallic Pd–Pt catalysts on

* Corresponding author.
E-mail address: vacange@ms.fci.unibo.it (A. Vaccari).

0021-9517/$ – see front matter
doi:10.1016/j.jcat.2004.01.024

various supports [9–16]. It is supposed that the mechanism of the poisoning by S-containing compounds (mainly benzothiophenes) involves a strong chemisorption on the metal sites followed by its hydrogenolysis, with formation of H_2S, which probably gives rise to the formation of a stable and inactive M–S species, according to the equilibrium:

$$M + H_2S \Leftrightarrow M\text{–}S + H_2.$$

The equilibrium may shift to the left-hand side with the hydrogen pressure and/or when the physicochemical characteristics of the metal atoms are modified, leading to the formation of electron-deficient metal sites, which lowers the strength of the M–S bond.

The metal ions can be modified by alloying (for example, bimetallic Pd–Pt catalysts, [17–19]) and/or changing the acid properties of the support, upon interaction of the reduced metal with the Brønsted acid sites. In order to shed light on the influence of Brønsted acid sites on the thio-tolerance, many studies have been carried out on several acidic supports [20–22], suggesting that Pd and Pt become thio-tolerant when the metallic or bimetallic particles are supported on highly acidic zeolite [5,18,21,22]. However, high acidity is not wanted for the HYD reactions, since it favors the cracking reactions to useless low molecular weight (LMW) products, outside the diesel range (mainly gases, which have to be burned in heat exchangers of the refinery). On the other hand, the acid sites of the supports have been claimed to play a key role in the ring-opening reactions leading to high molecular weight (HMW) compounds, which are very useful products for improving the cetane number in diesel fuels. For example, Sato et al. [3] claimed a significant role of the acid sites in the hydrocracking of tetralin, which involved a series of isomerization and ring-opening steps. In a following paper [4], some of these authors reported that the reaction pathway in the initial period differed from the one registered later in the reaction, with the requirement of close relationship between the active sites of hydrogenation and cracking.

Reddy and Song [23] investigated some Al-MCM-41 samples synthesized using different Al sources and reported a direct correlation between acidity and hydrocracking activity. Since the trend was consistent with the amount of Al incorporated in the framework, these authors claimed that the hydrocracking activity was exclusively due to the acid sites. However, loading a 3 wt% of Pt, they observed a significant improvement in the hydrocracking activity, with the conversion at 350 °C that increased from 77 to 100%, and with Pt promoting further cracking reactions. More recently, Ali et al. [24] reported that stable hydrocracking and hydrotreating catalysts can be obtained by using as support for the metal pairs Ni–W or Ni–Mo a β-zeolite in combination with an amorphous silica–alumina. A balance of weak and strong acidities of β-zeolite provided control over cracking, while silica–alumina supported high surface area and bigger pores. Thus, it is noteworthy that both the intrinsic thio-resistance of the Pd–Pt pair and the specific incidence of metal-catalyzed hydrogenolysis reactions have not yet been investigated independently from the contribution of the acid sites of the support.

The aim of this work was to deeply investigate the specific activity and thio-tolerance of the Pd–Pt pair as a function of its composition, regardless of any foreign effect due to the acid sites of the support. To this end, different Pd/Pt pairs with atomic ratios ranging from 3.0 to 5.5 have been supported on a Mg/Al mixed oxide [Mg–Al(O)] obtained from a hydrotalcite-type (HT) precursor [25–27], having the general formula $[Mg_{1-x}Al_x(OH)_2]^{x+}\,(A^{n-}_{x/n})\cdot mH_2O$, where A^{n-} is the balancing anion. As reported in the literature, the HT compounds are useful precursors of many catalysts or catalyst supports [25–29] that have no Brønsted acid sites present in the structure [25,26,30,31]. These catalysts have been investigated in the vapor-phase hydrogenation of naphthalene (Fig. 1), which was chosen as a model reaction for

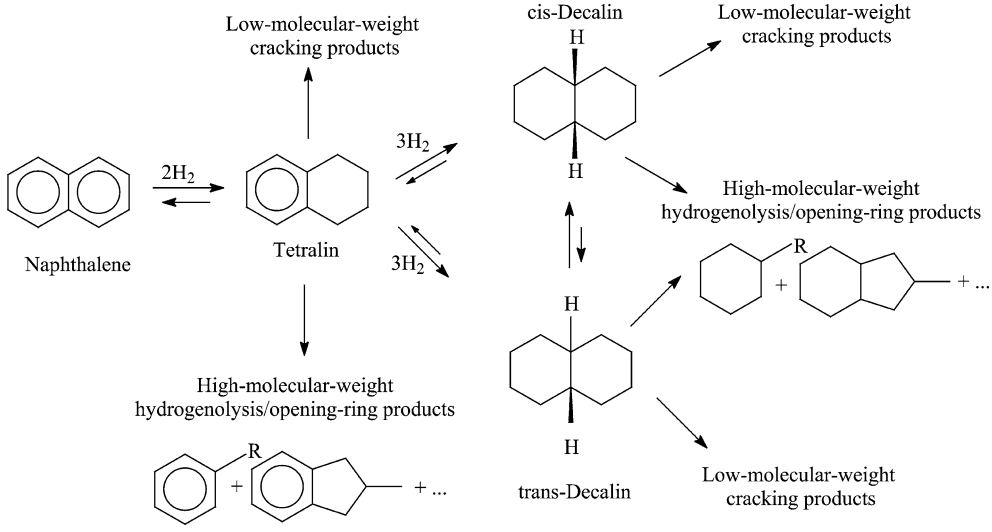

Fig. 1. Proposed reaction pathway for the vapor-phase hydrogenation of naphthalene.

the HYD of light cycle oil (LCO) feed in the modern refinery. Finally, the state of dispersed metal particles at the catalysts surface has been characterized by FTIR spectroscopy, using CO as a probe molecule. Results obtained from CO adsorption over reduced bimetallic catalysts and, for comparison, over the corresponding monometallic catalysts are reported here.

2. Experimental and methods

The Mg–Al(O) mixed oxide was prepared by calcination at 650 °C for 12 h of a commercial HT precursor by SASOL (D) ($Mg^{2+}/Al^{3+} = 2.26$ as atomic ratio; surface area 214 m^2/g) synthesized by hydrolysis using water excess at $30\,°C < T < 90\,°C$ of a mixture of Mg^{2+}- and Al^{3+}-alcoholate [32]. The Mg–Al(O) support showed a surface area of 95 m^2/g and a pore volume, determined by incipient wetness impregnation carried out with toluene, of 1.8 ml/g. The Pd/Pt (1 wt% of metals as compared to the total weight) on Mg–Al(O) catalysts, with different Pd/Pt atomic ratios (Table 1), were prepared by incipient wetness impregnation, using the right amount of Pd- and Pt-acetilacetonates (Aldrich) dissolved in toluene, to avoid any modification and/or acidification of the support. After impregnation, the catalysts were calcined at 500 °C for 4 h, grinded, and shaped to a 20- to 40-mesh particle size.

XRPD patterns were recorded on a Philips PW 1050/81 goniometer, equipped with a PW 1710 unit, using Cu-K_α radiation ($\lambda = 0.15418$ nm, 40 kW, 25 mA). N_2 sorption experiments at −196 °C were carried out with a Carlo Erba Sorpty 1750 instrument and specific surface area values were calculated using the BET method. FTIR spectra have been recorded by a Nicolet Nexus instrument, using conventional IR cells connected to a gas manipulation apparatus. The catalyst pure powders CAT1 and CAT3 (having the highest and the lowest Pd/Pt ratio, respectively) have been pressed into self-supporting disks, with an average weight of 30 mg. Before CO adsorption experiments, each fresh sample has been submitted to an "in situ" reduction treatment consisting in heating in pure hydrogen (53 kPa) at 300 °C, followed by outgassing at the same temperature in the IR cell itself. In another set of experiments, CO was adsorbed over catalyst pure powders after the reaction tests, either pretreated in vacuum at 300 °C or pretreated in hydrogen as reported above for the fresh powders. CO adsorption has been performed at room temperature, and spectra have been recorded at increasing CO partial pressure and after outgassing the samples at room temperature.

Table 1
Composition and BET surface area values (before and after reaction) of the catalysts investigated

Sample	Pd/Pt	Surface area (m^2/g)	
	atomic ratio	Before reaction	After reaction
CAT1	5.5	129	130
CAT2	4.0	126	122
CAT3	3.0	116	113

The catalytic tests were performed at 6.0 MPa (if not otherwise specified $H_2/N_2 = 1/1$ v/v) and in the 220–340 °C range using a stainless-steel tubular reactor (i.d. 8 mm, length 54 cm), heated by an electric oven controlled by two J thermocouples. Catalysts (6 cm^3, 14–20 mesh) were employed, located in the isothermal zone of the reactor. During the tests, the catalyst temperature was controlled using a 0.5-mm J thermocouple sliding in a stainless-steel capillary tube inside the catalytic bed. Before the tests, the catalyst was activated in a 200 ml/min flow of H_2, using a programmed increase of the temperature from room temperature up to 450 °C. The solution of naphthalene in *n*-heptane (10 wt%) was fed using a HPLC Jasco 880-PU pump, in a gas flow of a H_2/N_2 mixture (if not otherwise specified 1/1 v/v). Each catalytic test was performed for 5 h, collecting the products in a trap cooled to −10 °C after a preliminary period of 1 h, under the same conditions, to achieve steady-state activity. The quantitative analysis of the reaction products was carried out using a Carlo Erba GC6000 gas chromatograph, equipped with FID and a wide-bore PS264 column (5% methylphenylsilicone, length 25 m, inner diameter 0.53 mm, film width 1.5 μm). The products were preliminary and tentatively identified by GC-MS using a Hewlett–Packard GCD 1800 system equipped with a HP5 column (5% of methylphenylsilicone, length 25 m, inner diameter 0.25 mm, film width 0.25 μm) comparing the experimental GC-MS pattern with those present in the instrument library. Wide ranges of reaction conditions were investigated (temperature, contact time, H_2/naphthalene ratio); furthermore, since all the hydrotreated feeds contain small amounts of sulfur compounds responsible for catalyst poisoning, the thio-resistance of the catalysts was also investigated by feeding increasing amounts of dibenzothiophene (DBT) and benzothiophene (BT), representative of the S-containing molecules usually present in the industrial feeds.

3. Results and discussion

3.1. Catalyst characterization

The SEM replica (Fig. 2) shows a similar surface morphology for the HT precursors and the Mg–Al(O) mixed oxide obtained by calcination, in agreement with that previously reported in the literature [33]. The HT precursor showed a regular texture, with uniformly sized particles (Fig. 2A). More in detail (Fig. 2B), the sample exhibits a "brain-like" surface morphology, helpful to anchor the Pd/Pt active phase by incipient wetness impregnation. The XRPD of the catalysts before and after reaction (Fig. 3) show only the typical pattern of the Mg–Al(O) mixed oxide [25–27], without any evidence of oxide- or metal-segregated phases, an index of a very good and stable dispersion of the Pd/Pt

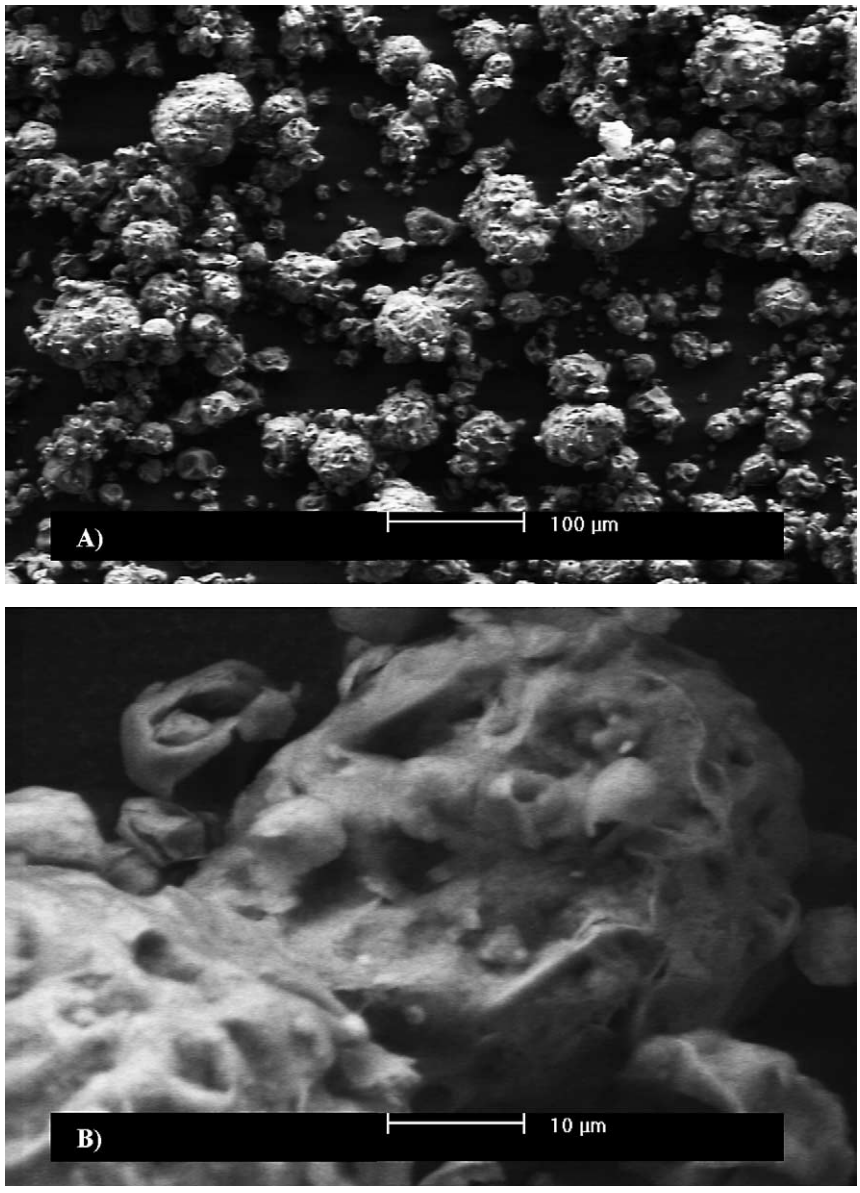

Fig. 2. SEM replica of the HT precursor.

pair, regardless of its composition. Finally the BET surface area values (Table 1) do not show any relevant loss of surface area after reaction, confirming the absence of segregation phenomena and/or significant deposition of heavy compounds (tar) on the surface.

3.2. FTIR characterization by CO adsorption

3.2.1. Samples before the catalytic tests

CO adsorption at room temperature over the reduced CAT1 sample (Pd/Pt = 5.5 as atomic ratio) gives rise to the spectra reported in Fig. 4A, recorded at increasing CO partial pressures (Fig. 4A, spectra a and b), in the presence of 132.5 Pa of CO (Fig. 4A, spectrum c), and after outgassing at room temperature (Fig. 4A, spectrum d). In the presence of CO, the spectrum consists of a quite broad and strong band centered at 2077 cm^{-1}, with a "tail" toward lower wavenumbers, and of a broad absorption around 1950 cm^{-1}, with a shoulder at 1880 cm^{-1}. CO gas in the IR cell is also evident and characterized by the weak PQR rotovibrational band at 2143 cm^{-1}. After outgassing at room temperature (Fig. 4A, spectrum d) there is a significant decrease in intensity of the higher frequency band, together with a pronounced shift toward lower frequencies, which leads to the detection of a peak at 2070, and an additional shoulder at 2030 cm^{-1}. The complex band at lower frequencies remains almost unchanged.

The spectra of CO adsorbed over a CAT3 catalyst (Pd/Pt = 3.0 as atomic ratio) under the same conditions (Fig. 4B, spectra a–c) show, again, an intense peak centered at 2082 cm^{-1} and a broad absorption below 2000 cm^{-1}, with a clear maximum at 1964 cm^{-1} and a shoulder at

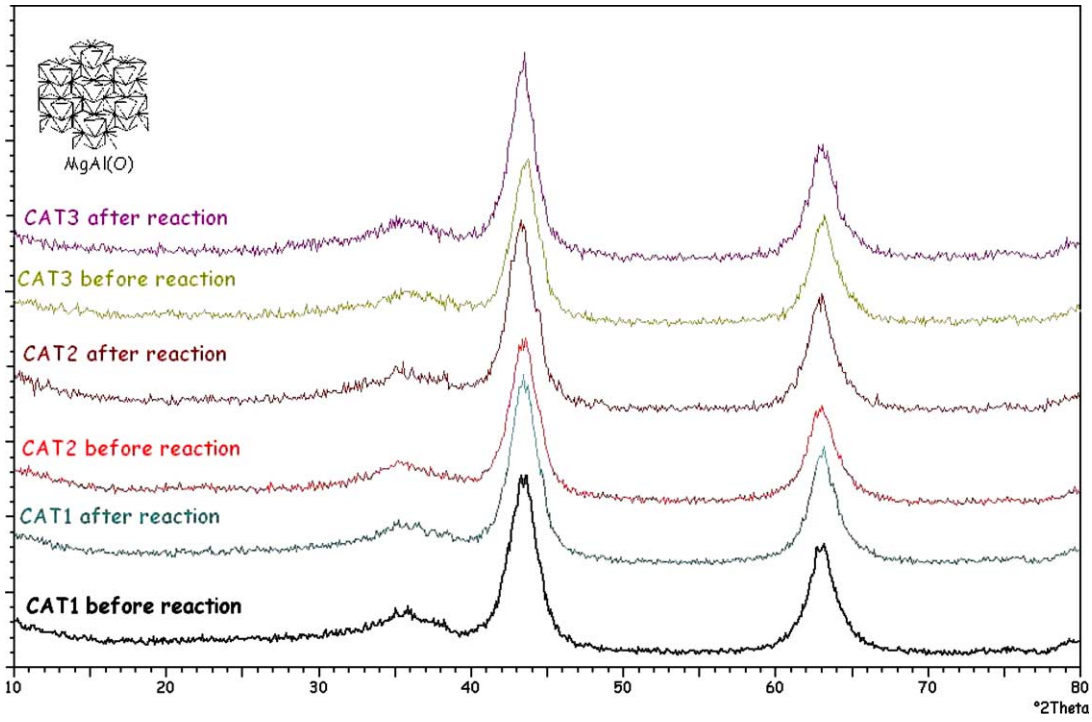

Fig. 3. XRD patterns of the investigated catalysts.

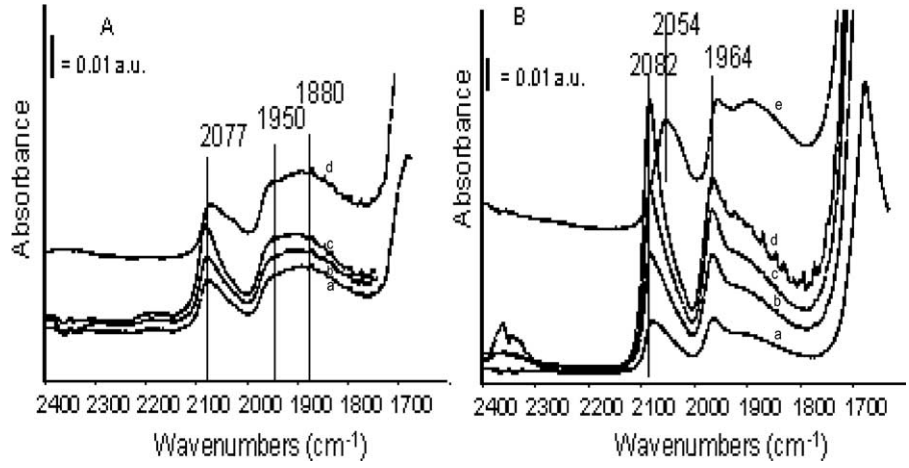

Fig. 4. FTIR spectra of CO adsorbed at room temperature over reduced CAT1 catalyst (A): at increasing CO partial pressure (a, b), in the presence of 132.5 Pa CO (c), after outgassing at room temperature (d), and FTIR spectra of CO adsorbed over reduced CAT3 catalyst (B): at increasing CO partial pressure (a, c), in the presence of 132.5 Pa CO (d), after outgassing at room temperature (e).

1880 cm^{-1}. In the spectrum recorded following outgassing at room temperature (Fig. 4B, spectrum e), a shift of the main band from 2082 to 2054 cm^{-1} may be observed. In addition, this band appears to be now more complex but, unlikely in the CAT1 spectra, not resolved in its components. In both samples, after outgassing, the broad absorptions below 2000 cm^{-1} are definitely more intense as compared to the band around 2080–2070 cm^{-1}. According to literature data the carbonyl stretching bands in the region 2085–2070 cm^{-1} are typically due to terminal carbonyl species linearly coordinated over reduced metal centers, which can be either Pd^0 or Pt^0 species, both present at the surface. Similar peak values have been detected by IR spectroscopy after CO adsorption on bimetallic palladium–platinum systems supported over different surfaces, such as NaY zeolite (νCO at 2085 cm^{-1}) [34], H-beta zeolite (νCO at 2087 cm^{-1}) [35], or silica–alumina (νCO at 2104 cm^{-1}) [11]. The slightly lower frequency we detected for the corresponding bands in our case, mainly in the CAT1 spectra, can be explained by taking into account the interaction of metallic particles with the strongly basic negative oxygen atoms of the Mg–Al(O) support [36]. According to the literature, this interaction is stronger than usual, due to electron density transfer from lattice basic oxygen ions to metal particles, and results in an

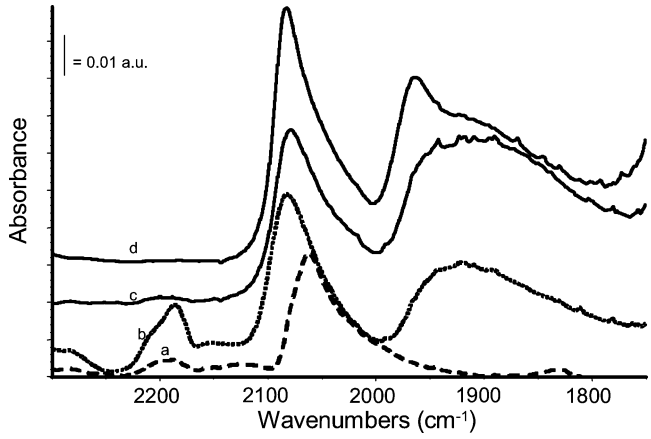

Fig. 5. FTIR spectra of 132.5 Pa CO adsorbed at room temperature over reduced Pt 1% on Al–Mg(O) sample (a), over reduced Pd 1% on Al–Mg(O) sample (b), and, for comparison, over CAT1 catalyst (c) and CAT3 catalyst (d).

improved backdonation from metal to CO. The band pattern below 2000 cm^{-1} corresponds to carbon monoxide adsorbed in bridging structures [37] and will be further discussed below.

In order to evaluate the effect of bimetallic particle formation at the catalyst surface, we also studied by IR spectroscopy the adsorption of 132.5 Pa of CO over the monometallic Pd and Pt samples, supported on Mg–Al(O) (Fig. 5, spectra a and b). CO adsorbed over metallic Pt has been reported to strongly favor the on-top position, due to electronic factors [38]. In agreement, it may be detected in Fig. 5, spectrum a, one broad and strong band at 2060 cm^{-1}, assigned to on-top coordinated species, and a very weak absorption around 1840 cm^{-1}, assigned to bridging species [37]. After outgassing at room temperature, there is a shift in the position of the main band down to 2050 cm^{-1} (spectrum not shown in Fig. 5), which is usually explained by the decreasing of dipole–dipole interaction between adjacent CO molecules at decreasing coverage. A similar shift, together with the detection of two or three different bands in the range 2020–1930 cm^{-1}, has also been reported by Gandao et al. [39] and Kazansky et al. [40], for CO adsorption on Pt supported over Mg–Al(O). They assigned these low-frequency components to CO on top on different forms of metallic particles having a very low coordination state (i.e., in corners or edges) or negatively charged, thus always strongly interacting with basic oxygen atoms of the support. In our samples none of those components has been detected, suggesting the presence of an almost homogeneous population of Pt particles, whose interaction with the support does not result in the formation of negatively charged particles. CO adsorption over Mg–Al(O)-supported Pd (Fig. 5, spectrum b) leads to the detection of a main band at 2080 cm^{-1} (linearly coordinated CO) and a broad band around 1940 cm^{-1} (bridged coordinated CO), thus showing a pattern which is very close to the one observed in the spectrum of CO adsorbed over the bimetallic samples (Fig. 5, spectra c and d), especially over a CAT1 sample having the highest Pd content. Outgassing at room temperature allows the shift of the main band toward lower wavenumbers (2074 cm^{-1}), but still, no bands possibly due to negatively charged Pd particles are detected. Another weak feature around 2180 cm^{-1} in both Pt and Pd catalysts spectra is assigned to CO coordinated over Al^{3+} ions of the exposed support.

From the above data, we can conclude that the broad and complex band below 2000 cm^{-1} in the spectra of bimetallic catalysts nicely corresponds to the bridging form of CO adsorbed over Pd metal particles. This assignment can be further confirmed by taking into account the integral band intensity ratio: *bridging CO species (absorbance arbitrary units)/linear CO species (absorbance arbitrary units)*, which decreases in the bimetallic catalyst from 1.99 (CAT1 Pd/Pt = 5.5) to 1.04 (CAT3 Pd/Pt = 3.0), thus exactly by a factor of 1.8, corresponding to the decrease from 5.5 to 3.0 in the Pd/Pt atomic ratio. This implies a "dilution" effect of the Pt atoms, which should exclusively increase the linear CO adsorbed fraction, thus Pd–Pd bonds are decreased in number by Pd–Pt bonds formation. The detection of at least two components in the bridging CO stretching band is well evident in CAT3 spectra at 1964, strong, and 1920 cm^{-1}. A Pd_2CO bridging carbonyl species over (100) planes of Pd crystals has been reported at 1963 cm^{-1}, while the bridging species over the (111) planes was proposed to absorb at lower wavenumbers (1936 and 1915 cm^{-1}) by Pawelec et al. [11], following CO adsorption on Pd and Pd/Pt supported over acid zeolites. Moreover, the occurrence of threefold coordinated species cannot be excluded, taking into account the broad absorption component below 1900 cm^{-1} [37]. From these data it seems likely that at the CAT3 surface there is an enrichment of Pd (100) planes (atoms at lower coordination with respect to (111)).

From the reported spectroscopic data the following remarks originate:

1. Compared to the monometallic samples, the spectra of CO over bimetallic Pd–Pt samples are not the simple superimposition of the single metal spectra. Certainly, the surface is significantly Pd rich; thus, infrared features reflect mainly the presence of CO adsorbed over Pd particles (see spectra of CAT1, Figs. 4A and 5), but the contemporary presence of Pd and Pt at the metal particle surface can be revealed by an enlargement of the band due to linearly adsorbed CO and a modification of the bridging carbonyl signal, well evident in CAT3 spectra (Figs. 4B, 5, and 6).
2. It is difficult to evaluate any electronic effects resulting from an alloying of the two metal phases at the surface. Rades et al. [34] proposed an IR study of CO adsorbed over a supported Pd–Pt (1:1) system indicating two main effects of alloy formation on metal–carbonyl spectra:
   (i) a ligand effect, which results in a shift downward for the linearly coordinated CO peak in the bimetallic

sample spectrum, with respect to the spectra of CO over pure components, and

(ii) a band intensity redistribution effect, characteristic of CO adsorption on adjacent metallic sites with different properties.

In both CAT1 and CAT3 samples we detected only a very slight shift of the linear CO peak toward lower frequencies with respect to pure Pd catalysts (ligand effect). On the other hand, an indication of alloying formation could be found in the spectra recorded after outgassing at room temperature, where the main band at 2077 cm^{-1} is shifted to 2070 cm^{-1} with a shoulder at 2030 cm^{-1} (CAT1, Fig. 4A, spectrum d) and the band at 2082 cm^{-1} is shifted to 2054 cm^{-1} (CAT3, Fig. 4B, spectrum e). This band might correspond to Pt^0–CO linear complexes, thus revealing a redistribution effect.

Some evidence of negatively charged metallic Pt particles can also be found in CAT1, (Figs. 4A and 5) characterized by the weak shoulder at 2030 cm^{-1} in the spectrum recorded after CO adsorption and outgassing. These species are known to decrease the catalyst sulfur resistance [40], and CAT1 is actually the sample most affected by the increasing amount of S-containing compounds in the feed (see Section 3.3).

3.2.2. Samples after the catalytic tests

The IR spectra of the samples after the catalytic tests, recorded in vacuum at increasing temperatures, point out the presence of adsorbed carbonate species stable up to 350 °C (not shown in Fig. 6) and of some residual organic surface species, characterized by CH stretching detectable around 3000 cm^{-1}, which are typical of saturated and unsaturated hydrocarbons (Fig. 6, inset). CO adsorption over the same surface (Fig. 6, spectrum a) leads mainly to the detection of carbonyl species coordinated on top over metal centers: these are characterized by a quite broad band around 2060 cm^{-1} significantly weakened as compared to the fresh, reduced sample (Fig. 6, spectrum c). The peak position shift (2060 cm^{-1} vs 2082 cm^{-1} in the fresh, reduced sample) can be due to a decrease in dipole/dipole coupling caused by poisoning of sites and/or electron donation from unsaturated adsorbed residual species to metal particles (as reported in the case of a Cu–Rh bimetallic supported catalyst [41]). The band due to bridging carbonyl species appears very weak and quite complex, centered below 1900 cm^{-1}, pointing out that CO adsorption in the twofold coordination configuration is strongly inhibited.

Treatment of the same surface in hydrogen at 300 °C (Fig. 6, spectrum b) and 400 °C failed to regenerate the same CO adsorption sites detected in the fresh, reduced sample (Fig. 6, spectrum c). Particularly, bridged species are not restored even after treatment in hydrogen at increasing temperatures. This effect can be due to the even smaller metal particles dimensions (higher dispersion) reached after catalytic activity.

3.3. Catalytic performances

First, attention was focused on the sample with a Pd/Pt atomic ratio equal to 4.0 (CAT2). In fact, this ratio has been claimed in the literature for the catalysts prepared using acid supports (crystalline or amorphous) as the most active in the hydrogenation and hydrogenolysis/ring-opening reactions and stable toward S-containing compounds [5,19,22]. Detailed results of the catalytic tests carried out on CAT2 (1.0 wt%; Pd/Pt = 4.0 as atomic ratio) feeding naphthalene under different reaction conditions are shown in Table 2. At 260 °C, this sample shows a complete conversion of naphthalene, mainly to decahydronaphthalene (DeHN or decalin, *cis* + *trans*) (yield > 80%), together with an appreciable amount of HMW compounds, mainly alkylcyclohexanes, relevant since they have high cetane numbers [42]. Considering the absence of Brønsted acid sites, these latter must

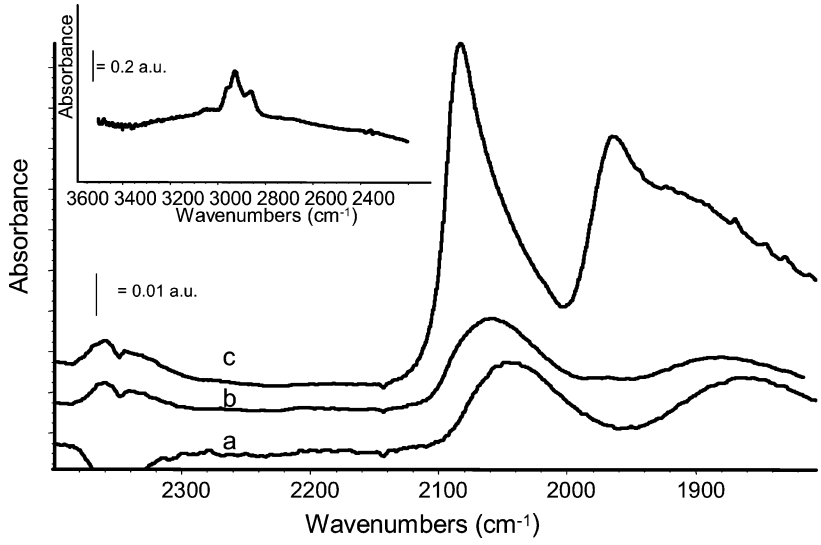

Fig. 6. FTIR spectra of 132.5 Pa CO adsorbed at room temperature over CAT3 after catalytic tests and following outgassing at 300 °C (a), over CAT3 after catalytic tests and hydrogen treatment at 300 °C in the IR cell (b), over fresh, reduced CAT3 (c). Inset: catalyst surface after activity tests: CH stretching region.

Table 2
Catalytic activity of CAT2 (1.0 wt%; Pd/Pt = 4.0 as atomic ratio) as a function of the reaction conditions

	Conversion of naphthalene (%)	Yield in Tetralin (%)	Decalin (*cis* + *trans*) (%)	HMW products (%)	C balance losses (%)
Temperature[a] (°C)					
260	99.9	3.6	83.5	15.3	0.0
300	97.4	10.2	68.9	18.2	0.1
340	76.2	20.0	40.9	15.6	0.0
260	99.2	8.1	77.5	13.2	0.3
Contact time[b] (s)					
6.8	99.9	3.6	83.5	15.3	0.0
3.4	99.2	8.0	76.6	13.1	1.6
1.7	97.5	69.0	14.4	8.6	5.5
H_2/naphthalene ratio[c] (mol/mol)					
21.0	99.9	3.6	83.5	15.3	0.0
16.5	97.5	43.6	39.9	14.7	0.0
12.0	93.8	49.7	28.6	13.4	2.1
DBT[d] (wt ppm)					
0	97.4	10.2	68.9	18.2	0.1
100 (17 wt ppm S)	98.7	9.6	66.3	20.3	2.5
1000 (170 wt ppm S)	98.6	9.0	59.4	22.1	8.1
3000 (510 wt ppm S)	92.4	23.4	54.1	14.2	0.7
0	96.7	10.4	70.1	18.7	0.0
BT[d] (wt ppm)					
0	96.7	10.4	70.1	18.7	0.0
73 (17 wt ppm S)	98.3	8.7	70.5	14.1	5.0
730 (170 wt ppm S)	96.7	6.9	56.6	19.8	13.4
2190 (510 wt ppm S)	95.8	18.0	61.7	10.2	5.9
0	95.4	12.1	70.6	10.0	2.7

[a] Contact time, 6.8 s; LHSV, 1 h^{-1}; H_2/naphthalene ratio, 21 mol/mol.
[b] Temperature, 300 °C; H_2/naphthalene ratio, 21 mol/mol.
[c] Temperature, 300 °C; contact time, 6.8 s; LHSV, 1 h^{-1}.
[d] Temperature, 300 °C; contact time, 6.8 s; LHSV, 1 h^{-1}; H_2/naphthalene ratio, 21 mol/mol.

be attributed only to hydrogenolysis reactions, catalyzed by the bimetallic Pd–Pt pair. The increase in the reaction temperature up to 340 °C causes a worsening of the naphthalene conversion and yield in decalin (*cis* + *trans*), in agreement with the exothermic character of the hydrogenation reactions. However, the increasing yield in tetralin is a more sensible index of deactivation than the decrease of naphthalene conversion, since tetralin is more thermodynamically stable than naphthalene. It must be noted that the losses in the carbon balance are very low regardless of the reaction temperature investigated, in agreement with the absence of reactions (polymerization, cracking, etc.) catalyzed by Brønsted acid sites. The formation of HMW compounds seems not to be affected by the reaction temperature, since the yield values remain almost constant throughout the entire temperature range investigated, confirming that they are formed essentially by metal-catalyzed hydrogenolysis. Finally, repeating the test at 260 °C, the catalyst almost completely recovered the starting performances, highlighting a good stability under the reaction conditions.

The progressive decrease of the contact time down to 1.7 s, favors mainly the first hydrogenation step to tetralin, while consecutive reactions (hydrogenation to decalin, *cis* + *trans*, or hydrogenolysis reactions) do not have sufficient time to occur. Also the decrease of the H_2 excess from more than four times the stoichiometric ratio (H_2/naphthalene = 21 mol/mol) to 2.5 times (H_2/naphthalene = 12 mol/mol) causes a worsening of the hydrogenation to decalin (*cis* + *trans*), while the yield in tetralin considerably increases, highlighting that the hydrogenation of naphthalene requires a H_2 content significantly higher than that required by the reaction stoichiometry. However, also under these conditions, the losses in the carbon balance remained very low, confirming the role of the acid sites in the formation of tar and low molecular weight useless products.

Finally, the thio-tolerance of CAT2 was investigated by adding increasing amounts of either dibenzothiophene or benzothiophene in the feed (maintaining constant the S content, for example, 100 wt ppm of DBT is equal to 73 wt ppm of BT and corresponds to 17 wt ppm of S ca.). It is noteworthy that 510 wt ppm of S (corresponding to 3000 wt ppm of DBT) is more representative of sulfur concentration in typical LCO feeds than low sulfur levels. This was done in order to obtain wider information on the poisoning by S-containing compounds. Surprisingly, the catalytic performances of this catalyst only slightly decreases on increasing the amount of DBT fed and the initial activity is fully recovered by removing the DBT from the feed. These very good results are confirmed by also feeding BT, highlighting that the catalytic performances of CAT2 are not notably affected by the S-containing compounds which are usually present in a LCO feed. This surprisingly high thio-tolerance is in contrast with the role claimed for the acid sites of the support [5,18,21] and may be attributed to the high hydrogenation activity of CAT2, that favors the hydrodesulfurization of both DBT and BT, probably through a hydrogenation pathway, as shown by the by-products detected (1,1′-bicyclohexylbenzene and cyclohexylbenzene) [43]. This hypothesis is in agreement with the rapid deactivation observed when analogous tests were performed at atmospheric pressure (i.e., under conditions in which hydrogenation reactions are thermodynamically unfavored).

To obtain data of the widest interest, the role of the Pd/Pt atomic ratio has been investigated. To this end, CAT1 (1.0 wt%, Pd/Pt = 5.5 as atomic ratio) and CAT3 (1.0 wt%, Pd/Pt = 3.0 as atomic ratio) were tested under the same reaction conditions and show behaviors similar to that of CAT2 (Table 3). The activity of both catalysts is not significantly affected by the reaction temperature. CAT1 shows a high hydrogenation activity (yield in decalin, *cis* + *trans*, higher than 90%), but HMW compounds are not formed. On the contrary, CAT3 has a lower naphthalene conversion and decalin (*cis* + *trans*) formation, with higher yields in tetralin and HMW compounds. Thus, the hydrogenation of naphthalene seems to be favored mainly by Pd, while Pt catalyzed the hydrogenolysis reactions. CAT1 is the sample most af-

Table 3
Catalytic activity as a function of the reaction temperature and thio-resistance of CAT1 (1.0 wt%; Pd/Pt = 5.5 as atomic ratio) and CAT3 (1.0 wt%; Pd/Pt = 3.0 as atomic ratio)

	Conversion of naphthalene (%)	Yield in Tetralin (%)	Decalin (*cis* + *trans*) (%)	HMW products (%)	C balance losses (%)
Temperature[a] (°C)					
CAT1					
260	98.4	5.2	88.0	0.2	5.0
300	98.9	1.7	92.1	0.1	4.9
340	99.4	1.4	92.4	0.1	5.6
260	99.7	1.5	91.7	0.2	6.3
CAT3					
260	95.3	9.7	56.6	21.4	7.6
300	93.9	8.4	62.3	18.5	4.6
340	89.8	9.0	58.6	17.2	5.1
260	95.4	10.7	58.1	19.4	7.1
DBT[b] (wt ppm)					
CAT1					
0	99.4	1.4	92.4	0.1	5.6
100 (17 wt ppm S)	99.6	2.9	94.9	0.2	1.6
1000 (170 wt ppm S)	97.9	24.3	67.8	0.1	5.7
3000 (510 wt ppm S)	98.8	51.8	41.0	0.1	5.8
0	99.6	11.2	84.5	0.1	3.8
CAT3					
0	95.3	9.7	56.6	21.4	7.6
100 (17 wt ppm S)	93.4	7.9	65.7	15.4	4.5
1000 (170 wt ppm S)	93.9	8.3	65.5	15.9	4.2
3000 (510 wt ppm S)	93.3	9.0	64.4	16.9	3.1
0	96.2	9.7	66.3	19.6	0.7

[a] Contact time, 6.8 s; LHSV, 1 h^{-1}; H_2/naphthalene ratio, 21 mol/mol.
[b] Temperature, 300 °C; contact time, 6.8 s; LHSV, 1 h^{-1}; H_2/naphthalene ratio, 21 mol/mol.

fected by increasing amounts of DBT in the feed (Table 3), while the activity of CAT3 does not decrease even upon feeding 3000 wt ppm of DBT (corresponding to 510 wt ppm wt of S). Therefore, if the content of Pt in the catalyst increases, the thio-tolerance also increases, in agreement with what was reported by Navarro et al. [9], who identified isolated electron-deficient Pt clusters on the Pd surface as responsible for the increased thio-tolerance.

In order to identify the optimum Pd/Pt atomic ratio, the Pd–Pt on basic Mg–Al(O) catalysts were compared in terms of productivity in decalin (DeHN) and hydrogenolysis (HMW) products both for kilogram (W) and liter (V) of catalyst (Fig. 7). The productivity per weight unit allows the specific activity of the active sites to be highlighted, reflecting also on the cost of the final catalyst. The productivity per volume unit is related to the dimensions of the reactor and represents the productivity of the industrial plant. All the catalysts form mainly hydrogenation products (DeHN), in agreement with both the absence of strong Brønsted acid sites and the mechanism of HMW compound formation reported in the literature [5,44]. However, it is noteworthy that by decreasing the Pd/Pt atomic ratio, the yield in hydrogenation products decreases, with a corresponding increase of that in HMW. Thus, Pd–Pt on basic Mg–Al(O) catalysts can be considered interesting catalysts for HDA reactions, with a reduced but not negligible activity in HMW formation and a very good thio-tolerance. The best compromise between hydrogenation (DeHN) and hydrogenolysis (HMW products) activity belongs to the catalyst with an intermediate Pd/Pt atomic ratio (4.0, CAT2).

4. Conclusions

The literature reports different hypotheses on the role of the acid sites and noble metals in the synthesis of HMW products and thio-tolerance, since both are always present in the catalysts investigated. To highlight the specific behavior of the Pt–Pt pair, which is one of the most promising reported in literature, both in the production of HMW compounds (hydrogenolysis/ring-opening) and in the thio-tolerance to increasing amounts of S-containing compounds, catalysts with different Pd/Pt atomic ratios were prepared by impregnation of a Mg/Al mixed oxide obtained by calcination of a commercial HT precursor, which has mainly basic sites.

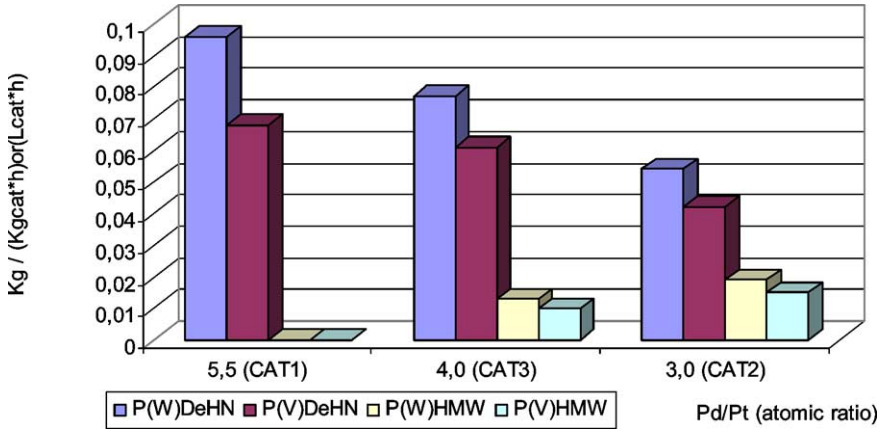

Fig. 7. Productivity in decalin (DeHN) and hydrogenolysis/ring-opening (HMW) products per kilogram (W) or liter (V) of catalyst for the Pd–Pt supported on Mg–Al(O) catalysts, with different Pd/Pt atomic ratios (temperature, 260 °C; contact time, 6.8 s; LHSV, 1 h^{-1}; H_2/naphthalene ratio, 21 mol/mol).

The samples CAT1 (1.0 wt%, Pd/Pt = 5.5 as atomic ratio), CAT2 (1.0 wt%, Pd/Pt = 4.0 as atomic ratio), and CAT3 (1.0 wt%, Pd/Pt = 3.0 as atomic ratio) were investigated to optimize the Pd/Pt ratio. The tests under different reaction conditions showed a high catalytic activity, mainly in hydrogenation products (decalin), in agreement with the absence of strong Brønsted acid sites. However, it is noteworthy that upon decreasing the Pd/Pt atomic ratio, the yield in hydrogenation products also decreased, with a corresponding increase in the yield of HMW compounds, thus highlighting a significant role also of the hydrogenolysis reactions, mainly catalyzed by Pt. Moreover, these samples did not form useless LMW cracking and/or heavy compounds (tar), in agreement with the absence of strong acid sites. The catalyst with the highest Pd/Pt atomic ratio (5.5) showed the highest hydrogenation activity and, following IR data, the highest backbonding effect (resulting in lower CO stretching frequency: 2077 vs 2082). So, taking into account that naphthalene interaction at the catalyst surface occurs mainly through π-bond formation, it seems likely that naphthalene is more tightly adsorbed (and hydrogenated) at this surface.

Finally, the thio-tolerance of these catalysts was investigated by feeding increasing amounts of dibenzothiophene (DBT) or benzothiophene (BT). These catalysts showed almost no effect even by feeding 3000 wt ppm of DBT (corresponding to 2190 wt ppm of BT or about 510 wt ppm of S). This surprising result is in contrast with the key role of acid sites claimed in the literature, highlighting an intrinsic thiotolerance of the Pd/Pt pair, mainly for higher Pt contents. Thus, Pd/Pt on basic Mg–Al(O) catalysts can be considered an interesting alternative for HDA, with a reduced but significant activity in the synthesis of HMW compounds by hydrogenolysis reactions mainly catalyzed by Pt. On the other hand, these results confirm the relevant role of acid sites in the HMW synthesis, very probably by isomerization–ring-opening paths [3]. Between the catalysts investigated, the best compromise between hydrogenation (decalin) and hydrogenolysis (HMW products) activity belongs to the catalyst with a Pd/Pt = 4.0 (as atomic ratio).

Acknowledgments

Financial support under Growth Project GRD2-2000-30316 is gratefully acknowledged. Thanks are due to SASOL (D) for supplying the commercial HT precursor.

References

[1] B.H. Cooper, A. Stanislaus, Catal. Rev. Sci. Eng. 36 (1994) 75.
[2] B.H. Cooper, B.B.L. Donnis, Appl. Catal. A 137 (1996) 203.
[3] K. Sato, Y. Iwata, T. Yoneda, A. Nishijima, Y. Miki, H. Shimada, Catal. Today 45 (1998) 367.
[4] K. Sato, Y. Iwata, Y. Miki, H. Shimada, J. Catal. 186 (1999) 45.
[5] H. Yasuda, Y. Yoshimura, Catal. Lett. 46 (1997) 43.
[6] R. Hernández-Huesca, J. Mérida-Robles, P. Maireles-Torres, E. Rodríguez-Castellón, A. Jiménez-López, J. Catal. 203 (2001) 122.
[7] C.H. Bartolomew, P.K. Agarwal, J.R. Katzer, Adv. Catal. 31 (1982) 135.
[8] J. Barbier, E. Lamy-Pitara, P. Marecot, J.P. Boitiaux, J. Cosyns, F. Verna, Adv. Catal. 37 (1990) 279.
[9] R.M. Navarro, B. Pawelec, J.M. Trejo, R. Mariscal, J.L.G. Fierro, J. Catal. 189 (2000) 184.
[10] A.D. Schmitz, G. Bowers, C. Song, Catal. Today 31 (1996) 45.
[11] B. Pawelec, R. Mariscal, R.M. Navarro, S. van Bokhorst, S. Rojas, J.L.G. Fierro, Appl. Catal. A 225 (2002) 223.
[12] M.J. Martínez-Ortiz, G. Fetter, J.M. Domínguez, J.A. Melo-Banda, R. Ramos-Gómez, Micropor. Mesopor. Mater. 58 (2003) 73.
[13] S.K. Maity, J. Ancheyta, L. Soberanis, F. Alonso, M.E. Llanos, Appl. Catal. A 244 (2003) 141.
[14] P. Afanasiev, M. Cattenot, C. Geantet, N. Matsubayashi, K. Sato, S. Shimada, Appl. Catal. A 237 (2002) 227.
[15] S. Albertazzi, R. Ganzerla, C. Gobbi, M. Lenarda, M. Mandreoli, E. Salatelli, P. Savini, L. Storaro, A. Vaccari, J. Mol. Catal. A: Chem. 200 (2003) 261.
[16] M. Jacquin, D.J. Jones, J. Roziére, S. Albertazzi, A. Vaccari, M. Lenarda, L. Storaro, R. Ganzerla, Appl. Catal. A 251 (2003) 131.
[17] J.L. Rousset, L. Stievano, F.J. Cadete Santos Aires, C. Geantet, A.J. Renouprez, M. Pellarin, J. Catal. 202 (2001) 163.
[18] H. Yasuda, T. Sato, Y. Yoshimura, Catal. Today 50 (1999) 63.
[19] T. Fujikawa, K. Idei, T. Ebihara, H. Mizuguchi, K. Usui, Appl. Catal. A 192 (2000) 253.
[20] L.J. Simon, J.G. van Omnen, A. Jentys, J.A. Lercher, Catal. Today 73 (2002) 105.
[21] H. Yasuda, N. Matsubayashi, T. Sato, Y. Yoshimura, Catal. Lett. 54 (1998) 23.
[22] N. Matsubayashi, H. Yasuda, M. Imamura, Y. Yoshimura, Catal. Today 45 (1998) 375.
[23] K.M. Reddy, C. Song, Catal. Today 31 (1996) 137.
[24] M.A. Ali, T. Tatsumi, T. Masuda, Appl. Catal. A 233 (2002) 77.
[25] F. Cavani, F. Trifirò, A. Vaccari, Catal. Today 11 (1991) 173.
[26] F. Trifirò, A. Vaccari, in: J.L. Atwood, J.E.D. Davies, D.D. MacNicol, F. Vögtle (Eds.), Comprehensive Supramolecular Chemistry, vol. 7, Pergamon, Oxford, 1996, p. 251.
[27] V. Rives (Ed.), Layered Double Hydroxides: Present and Future, Nova Science, New York, 2001.
[28] A. Vaccari, Appl. Clay Sci. 14 (1999) 161.
[29] F. Basile, G. Fornasari, A. Vaccari, in: A. Hubbard (Ed.), Encyclopedia of Surface and Colloid Science, Dekker, New York, 2002, p. 909.
[30] A. Corma, V. Fornés, R.M. Martín-Aranda, F. Rey, J. Catal. 134 (1992) 58.
[31] A. Vaccari, Catal. Today 41 (1998) 53.
[32] K. Diblitz, K. Noweck, A. Brasch, J. Schiefler, Eur. Patent 807,086 (1996).
[33] M.A. Ulibarri, I. Pavlovic, C. Barriga, M.C. Hermsín, J. Cornejo, Appl. Clay Sci. 18 (2001) 17.
[34] T. Rades, V.Yu. Borokov, V.B. Kazansky, M. Polisset-Thfoin, J. Fraissard, J. Phys. Chem. 100 (1996) 16238.
[35] J.-K. Lee, H.-K. Rhee, J. Catal. 177 (1998) 208.
[36] C. Goyhenex, M. Croci, C. Claeys, C.R. Henry, Surf. Sci. 352–354 (1996) 475.
[37] N. Sheppard, T.T. Nguyen, Adv. Infrared Raman Spectrosc. 75 (1978) 67.
[38] C. Hippe, R. Lambert, G. Schultz-Ekloff, U. Schubert, Catal. Lett. 43 (1997) 195.
[39] Z. Gandao, B. Coq, L.C. de Menorval, D. Tichit, Appl. Catal. A 147 (1996) 395.
[40] V.B. Kazansky, V.Yu. Borokov, A.I. Serykh, F. Figueras, Catal. Lett. 49 (1997) 35.
[41] J.A. Anderson, C.H. Rochester, Z. Wang, J. Mol. Catal. A: Chem. 139 (1999) 285.
[42] Shell Report No. 199.
[43] M. Breysse, G. Djega-Mariadassou, S. Pessayre, C. Geantet, M. Vrinat, G. Pérot, M. Lemaire, Catal. Today 84 (2003) 129.
[44] A. Corma, V. González-Alfaro, A.V. Orchillés, J. Catal. 200 (2001) 34.